ChemCatChem
The European Society Journal for Catalysis
Chemistry Europe
European Chemical Societies Publishing
Supported by GECATS GERMAN CATALYSIS SOCIETY

Accepted Article

Title: Tuning nano-nickel catalyst hydrogenation aptitude by on-the-fly zirconium doping

Authors: Małgorzata Zienkiewicz-Machnik, Ilona Goszewska, Damian Giziński, Anna Śrębowata, Katarzyna Kuzmowicz, Adam Kubas, Krzysztof Matus, Dmytro Lisovytskiy, Marcin Pisarek, and Jacinto Sa

This manuscript has been accepted after peer review and appears as an Accepted Article online prior to editing, proofing, and formal publication of the final Version of Record (VoR). This work is currently citable by using the Digital Object Identifier (DOI) given below. The VoR will be published online in Early View as soon as possible and may be different to this Accepted Article as a result of editing. Readers should obtain the VoR from the journal website shown below when it is published to ensure accuracy of information. The authors are responsible for the content of this Accepted Article.

To be cited as: *ChemCatChem* 10.1002/cctc.202000235

Link to VoR: https://doi.org/10.1002/cctc.202000235

WILEY-VCH

10.1002/cctc.202000235

WILEY-VCH

FULL PAPER

Tuning nano-nickel catalyst hydrogenation aptitude by on-the-fly zirconium doping

Małgorzata Zienkiewicz-Machnik*,[a] Ilona Goszewska,[a] Damian Giziński,[a] Anna Śrębowata,[a] Katarzyna Kuzmowicz,[a] Adam Kubas,[a] Krzysztof Matus,[b] Dmytro Lisovytskiy,[a] Marcin Pisarek,[a] and Jacinto Sá*[a, c]

Abstract: The effect of nano-Ni catalyst post-synthetic Zr-modification on hydrogenation reaction of 6-methyl-5-hepten-2-one was investigated in a fixed bed continuous-flow micro-reactor to produce fine chemicals. The catalytic performance revealed that Zr-doping achieved by surface organometallic chemistry approach modifies the natural aptitude of nickel to hydrogenate C=C bond, since the addition of small quantities of zirconium significantly increased the amount of unsaturated and saturated alcohols formed in 6-methyl-5-hepten-2-one hydrogenation. Quantum chemical calculations revealed a stronger interaction between Zr←O=C that promotes the formation of C=C semihydrogenation product and enhances the probability of complete hydrogenation. The on-the-fly strategy presented herein enables for rapid optimization and understanding of catalytic processes.

Introduction

In the past few decades, organic processes conducted under flow conditions have attracted growing attention due to significant benefits in respect to environmental compatibility, safety and efficiency. [1-4] In particular, chemoselective flow heterogeneous catalysis yields desired products without significant levels of by-product, avoiding costly, unsustainable and time-consuming purification processes. This feature enables flow processes to be assembled as a continuous multi-step workflow for the synthesis of fine chemicals. [5-7]

To fully capitulate the advantages offered by chemoselective flow heterogeneous catalysis, novel catalysts must be developed that can operate under the constrains of flow processes (e.g. minimum particle size, stable to mechanical stress, etc). Additionally, the new catalysts should be when possible made of transition metals, which are abundant and cheap. Our research efforts have been so far focused on hydrogenation reactions catalysed by nano-Ni catalysts supported on inert polymeric resins [8-10] and their alteration via on-the-fly surface modification [9,10] to increase the understanding of the processes and improve catalytic performance. We reported on the impact of particle accretion [9] and Sn-doping [10] on the activity and selectivity in the hydrogenation of α, β – unsaturated aldehydes and ketones. The obtained results showed that on-the-fly modification offers a simple workflow, cost-effective and adaptable strategy for process intensification and optimization. Catalyst surface alterations were achieved via surface organometallic chemistry (SOMC) route. [11,12]

Sn-doping of parent Ni catalyst decreased the stability of the adsorption complex and a switch of the thermodynamic order of the favoured products. [10] Spurred by these findings, we decided to extend our studies on the hydrogenation of 6-methyl-5-hepten-2-one to nano-Ni surface modification with zirconium. [10] Zirconium was selected as dopant due to its difference in the electronic structure including electronegativity compared to Ni and Sn, which allows exploring both, the geometric and electronic effects on hydrogenation of 6-methyl-5-hepten-2-one to produce fine chemicals. [13,14] Ultimately, the study aims to establish if the surface modifications and their impact in the catalysis can be assigned to tabulated parameters (e.g., electronegativity, atom radius, etc) or each element must be treated independently.

Results and Discussion

Nano-Ni parent catalyst ($NiTSNH_2$) was obtained at room temperature conditions, during one-pot, two-step synthesis where Ni NPs were grafted on the polymeric resin terminated with amino groups (TentaGel-S-NH_2, $TSNH_2$). [8-10] The metal content in $NiTSNH_2$ was found to be 0.68% wt. [8-10] For the modification of the parent catalyst with Zr we applied the procedure adopted to synthesize the Ni-Sn catalyst. [10] Shortly, Ni-Zr material was synthesised using ThalesNano H-Cube Pro™ flow micro-reactor via surface organometallic chemistry route. The bimetallic catalyst was subsequently flushed with ethanol to remove Zr ions excess and used in 6-methyl-5-hepten-2-one hydrogenation immediately after the preparation. The metals loading estimated for $NiZr_{0.12}TSNH_2$ by atomic absorption spectroscopy was found to be 0.74 wt%, where the subscript value corresponds to Ni/Zr atomic ratio.

PXRD diffraction pattern of the bimetallic catalyst was recorded and compared with the results reported previously [10] for the polymeric resin and the monometallic Ni catalyst. Obtained results show that the patterns are nearly the same (Fig. 1), with two diffraction peaks associated with the polymer structure. The lack of clear diffraction peak for metal nanoparticles is related to

---

[a] Dr M. Zienkiewicz-Machnik, I. Goszewska, Dr D. Giziński, Dr A. Śrębowata, K. Kuzmowicz, Dr A. Kubas, Dr D. Lisovytskiy, Dr M. Pisarek, Prof. J. Sá
Institute of Physical Chemistry, Polish Academy of Sciences
Kasprzaka 44/52, 01-224 Warsaw (Poland)
E-mail: mzienkiewiczmachnik@ichf.edu.pl, jacinto.sa@kemi.uu.se
[b] K. Matus
Institute of Engineering Materials and Biomaterials
Silesian University of Technology
Konarskiego 18 A, 44-100 Gliwice (Poland)
[c] Prof. J. Sá
Department of Chemistry, Ångström Laboratory
Uppsala University
Box 532, 751 20 Uppsala (Sweden)

Supporting information for this article is given via a link at the end of the document.

Accepted Manuscript

This article is protected by copyright. All rights reserved.

10.1002/cctc.202000235

the low metal loading but also to the small particles average size (estimated previously to be ca. 6.8 nm [10]). The polymeric diffraction peaks did not change with metal anchoring, as well as with the doping, which suggests that neither affects significantly the support structure. [6,10]

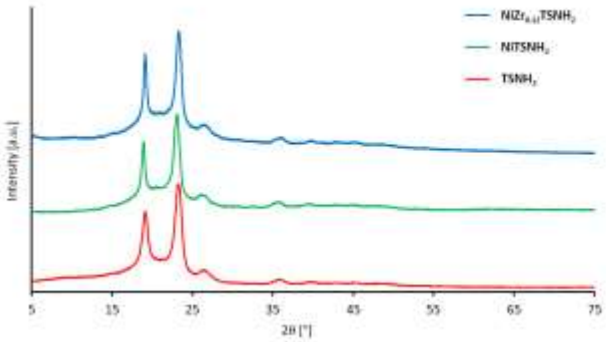

Figure 1. PXRD patterns for the polymeric resin, mono- and bimetallic catalysts.

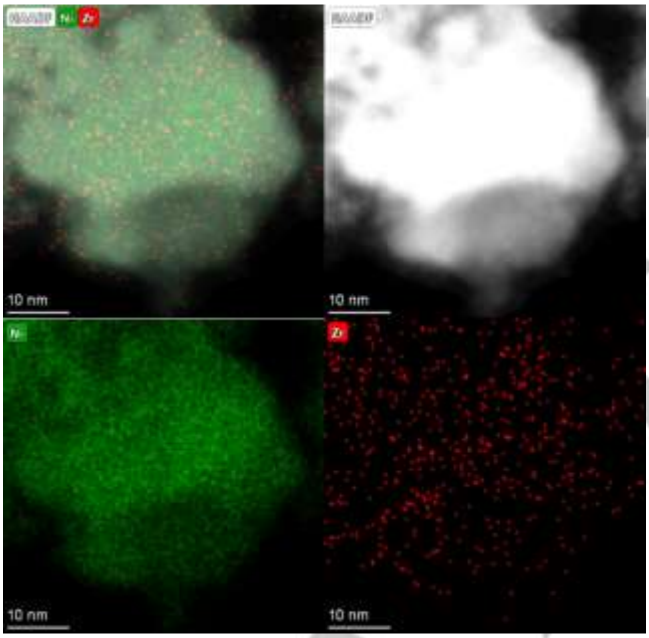

Figure 2. STEM images with EDS elemental mapping for $NiZr_{0.12}TSNH_2$.

Since the $NiTSNH_2$ used in this study is the same as the one reported elsewhere, [10] the TEM images are not reported but the Ni average particles size was estimated to be 6.8 nm. Zr-doping did not affect the Ni average particles size in a measurable way. To establish the presence of Zr on the surface of Ni, STEM analysis with EDS-elemental mapping was investigated for the doped catalyst (Fig. 2). We selected a large particle assemble region to assess that Zr is only found when Ni is presence. Fig. 2 shows clearly that Zr is evenly distributed on the nickel surface and absent when Ni is not present. Please take notice that the size of the Zr speckles is not associated with Zr size but to EDS pixel size and metal intensity.

XPS analysis was carried out to determine the oxidation state of Ni in the un- and -doped catalysts. Ni $2p_{3/2}$ XPS spectra of the catalysts (Fig. 3) are dominated by three signals ascribed to Ni^0 (maximum between 852 - 853 eV), [15] Ni^{3+} (maximum between 855 - 856 eV) [16] and Ni shake-up satellite (maximum between 860 - 861 eV). [15] We have in the past the signal between 855 - 856 eV associated to $Ni(OH)_2$ [10] based on the binding energy [17] but recent X-ray absorption spectroscopy (XAS) experiments revealed that the signal could not be fitted to a Ni^{2+} but rather to Ni^{3+}. [9] Our earlier studies also suggest that Ni^{3+} form is located primarily on the surface and is the product of surface passivation with atmospheric air, [9] which can be reduced partially or even fully to Ni^0 during the catalytic test. There was a good match of the XAS spectrum with Ni_2O_3 we suspect that its structure is different because Ni_2O_3 is not reducible at low temperature and somehow modulated/strained by the underlying Ni^0 structure. However, at present, we are unable to state what is the true structure and coordination status of the Ni^{3+} species. The ratio of Ni^0:Ni^{3+} was found to be roughly 1:3 for both samples. Zr $3d_{5/2}$ XPS region for the bimetallic Ni-Zr catalyst was fitted with a single component with a maximum at 182.4 eV associated with Zr^{4+} as ZrO_2. [18,19] The good match between the measured binding energy for Zr in the catalyst and the ZrO_2 reference prevents us from detecting any electron donation from Zr to Ni, meaning XPS analysis suggests minimal to no electron donation.

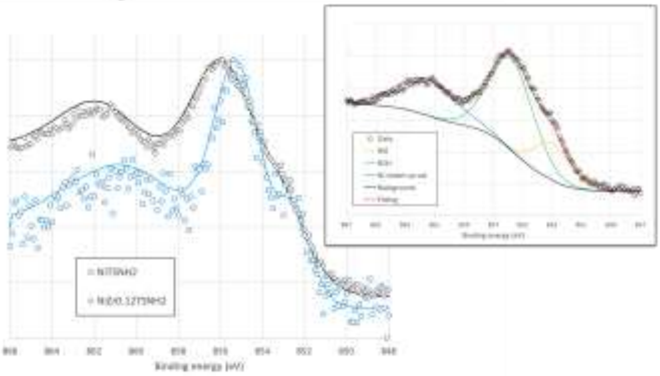

Figure 3. Ni $2p_{3/2}$ XPS region of $NiTSNH_2$ and $NiZr_{0.12}TSNH_2$. Insert fitting of the $NiZr_{0.12}TSNH_2$ signal.

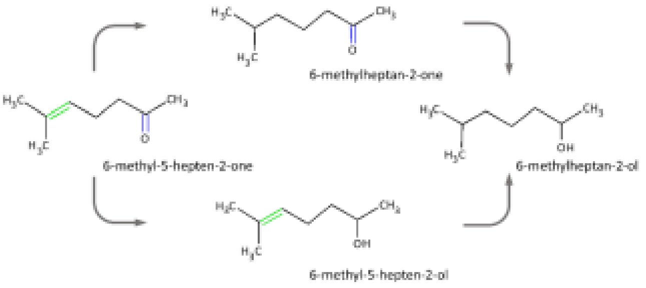

Scheme 1. The possible pathways for 6-methyl-5-hepten-2-one hydrogenation.

Accepted Manuscript

This article is protected by copyright. All rights reserved.

10.1002/cctc.202000235

Scheme 1 shows the reaction pathways for 6-methyl-5-hepten-2-one hydrogenation. Continuous-flow hydrogenations of 6-methyl-5-hepten-2-one were carried out under different conditions of temperature (25 – 100 °C) and pressure (10 – 60 bar) using H-Cube Pro™ micro-reactor. The catalytic experiment was conducted with a constant reactant flow rate (0.5 ml/min).

6-methyl-5-hepten-2-one hydrogenation over parent $NiTSNH_2$ yielded 100% selectivity toward saturated ketone formation and a substrate activity of ca. 21 μmol/min for a reaction conducted at 100 °C and 40 bar of H_2 (the optimum values of temperature and pressure).[10] The addition of small quantities of zirconium to the parent catalyst affected both activity and product selectivity. Starting with activity studies (Fig. 4), the addition of Zr led to at least twofold drop in activity no matter what temperature or H_2 pressure used, similar to what was found with Sn modification.[10] The general trend is that activity increases when reaction temperature and/or H_2 pressure increases. This is particularly noticeable for the experiments ran at 45 °C, where the catalytic activity is only detected when H_2 pressure reaches 60 bar.

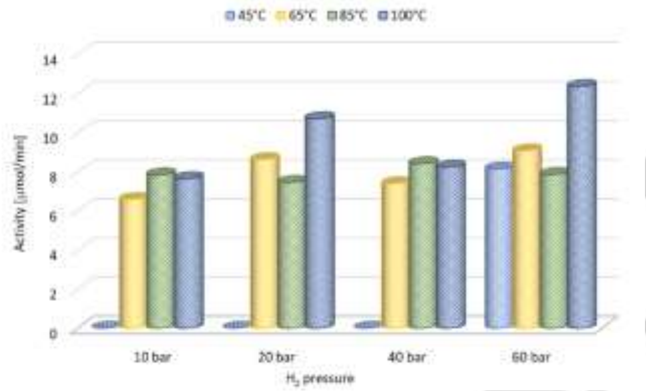

Figure 4. Dependence of the reaction conditions on 6-methyl-5-hepten-2-one catalytic activity over $NiZr_{0.12}TSNH_2$ with 0.5 ml/min flow rate of the reactant.

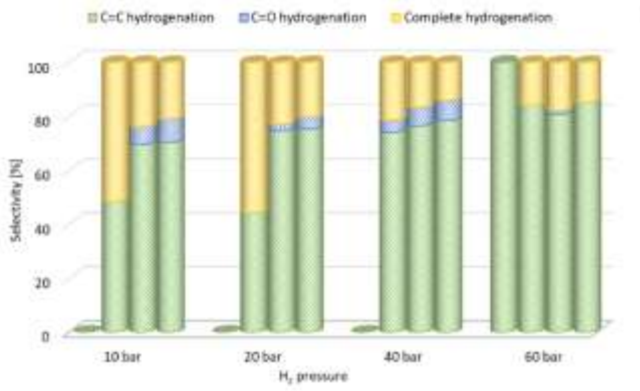

Figure 5. Effect of the reaction conditions on the selectivity of 6-methyl-5-hepten-2-one hydrogenation over $NiZr_{0.12}TSNH_2$ with 0.5 ml/min flow rate of the reactant.

The decrease in the catalytic activity of Sn-doped catalyst was connected with geometric blocking of the nickel surface.[10] On the basis of STEM with EDS and XPS analysis and the fact that Zr is inactive in the catalysis, the observed decrease in activity is rationalized as geometric blocking of the nickel surface, analogous to tin investigation.

Moreover, Zr doping modifies significantly the natural aptitude of nickel to hydrogenate C=C bond (Fig. 5). The addition of small amounts of zirconium results in the formation of other hydrogenation products, namely unsaturated alcohol and complete hydrogenation of 6-methyl-5-hepten-2-one. The formation of unsaturated and/or saturated alcohol is strongly dependent on the reaction conditions (Fig. 5). In most cases, both saturated ketone and saturated alcohol are formed in the catalysed reaction. Furthermore, the higher temperature (≥ 65 °C) causes the presence of all three hydrogenation products in the post-reaction solution whereas at lower temperature there is no unsaturated alcohol formation. Obtained data revealed that independently of Zr content, the formation of complete hydrogenation product is more favourable than the saturation of C=O bond. This finding can be assigned to the high adsorption strength of C=C hydrogenation product which leads to further saturation of the carbonyl group and the formation of complete hydrogenation product. It should be mentioned that the catalyst maintained the reported performance for 5h on stream. Moreover, EDXRF analysis of the post-reaction solutions had no measurable amount of metals what suggests the effect of active phase leaching is believed to be negligible. This was also confirmed by XPS analysis of the spent catalyst (Fig. 6 and S1), which shows no significant change in the metals content. Furthermore, XPS revealed that the electronic structures of Ni and Zr were preserved, confirming catalyst robustness.

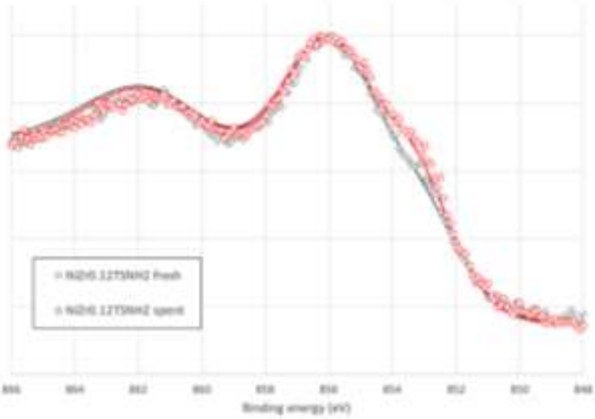

Figure 6. Ni $2p_{3/2}$ XPS region of $NiZr_{0.12}TSNH_2$ fresh and spent (after catalysis).

To comprehend further the structure-activity relationship, we evaluated the effect of substrate flow rate on the catalytic performance of Zr-doped material by carrying experiments with 0.3 and 1 ml/min substrate flow rates (Fig. 7 and S2-S5). Based on the obtained results for different substrate flow rates, it can be noticed that the catalytic activity increases in the following order: 0.3 ml/min < 0.5 ml/min << 1 ml/min. The observed trend was not anticipated and suggests reversible substrate poisoning. At low

Accepted Manuscript

This article is protected by copyright. All rights reserved.

10.1002/cctc.202000235

flow rates, the substrate is allowed to be on the surface for a longer period, leading to site saturation that blocks sites for H_2 activation. Contrastingly, at high flow rates, the sites cannot be fully saturated thus providing sufficient amounts of activated hydrogen to perform the hydrogenation reactions. The overall selectivity was not affected significantly, which is expected since the flows should not change meaningfully the catalytic aptitudes to specific bond hydrogenation, considering that the catalyst is stable throughout the reaction.

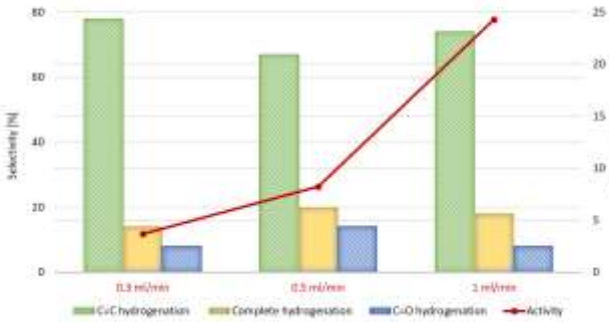

Figure 7. The reactant flow rate impact on catalytic performance of $NiZr_{0.12}TSNH_2$ in hydrogenation of 6-methyl-5-hepten-2-one. Reaction conditions: T = 100 °C, H_2 pressure = 40 bar.

According to our earlier studies, [10] the optimum conditions of temperature and H_2 pressure (100 °C, 40 bar) for 6-methyl-5-hepten-2-one hydrogenation were selected to evaluate the effect of Zr doping. Data summarised in Fig. 8 show that the catalytic activity, as well as the selectivity for the tested Ni-Zr bimetallic catalyst ($NiZr_{0.12}TSNH_2$) and the one with higher amount of Zr ($NiZr_{0.18}TSNH_2$), are nearly the same, independently on Zr concentration. This suggests that Zr decorates specific sites on Ni surface and once they are saturated the new Zr atoms will coordinate on top of the already existing ZrO_2. Since these atoms will have to direct contact with Ni they cannot affect its electronic and/or geometric structures, and thus cause no significant changes to the catalytic properties of the catalyst.

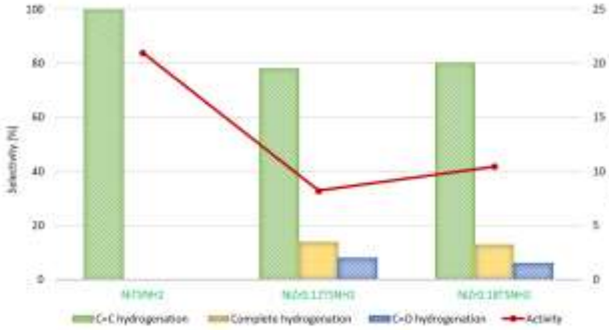

Figure 8. Comparison of the catalytic performance of the mono- and Zr-modified catalysts. Reaction conditions: T = 100 °C, H_2 pressure = 40 bar.

Quantum chemical calculations revealed that zirconium atom incorporates into the nickel lattice at the surface of model Ni_{13} species. The model adapted is analogous to the system adapted for Ni-Sn studies before. [10] This outcome is in line with recent computations on larger nickel clusters doped with light atoms. [20] Multiplicity of 7 was identified as the most stable spin state of the nanoparticle model Ni_{13}. Structures, where the zirconium replaced central atom or was kind of ad-atom (similarly to Sn), were found to be higher in energy by 11.3 or 32.3 kcal/mol, respectively. Zr atom incorporation influences Ni...Ni average interatomic distance that increases from 2.28 Å (Ni_{13}) to 2.30 Å ($Ni_{13}Zr$). Closest Ni...Zr contact is 2.47 Å. According to Löwdin population analysis, [21] Zr gains small positive charge of 0.13 a.u. while an average charge of nickel atoms is -0.01 a.u. Furthermore, four unpaired electrons of isolated Zr atom were found to be coupled antiferromagnetically with the nickel atoms (Zr spin population of -0.35, average Ni spin population of 0.49). The magnitude of coupling is large as the calculated expectation value of S^2 operator (12.21) does not deviate much from the expected value for six unpaired electrons (12.00).

According to Fig. 9, the interaction mode of the substrate with the catalyst species is similar for both undoped and doped catalysts, i.e. the interaction occurs via both C=O and C=C bonds. Small positive charge associated with Zr atom makes it better Lewis acid centre than Ni and carbonyl oxygen prefer interaction with zirconium atom over nickel atom (see inset in Figure 9). The binding energy of the substrate increases by 10.0 kcal/mol when going from Ni_{13} to $Ni_{13}Zr$ catalyst. The degree of substrate activation can be tracked back to changes in C=C and C=O bond lengths that are 1.36 and 1.22 Å for isolated substrate, respectively. The carbon-carbon double bond is elongated by 0.05 Å for Ni_{13} and 0.07 Å in the case of $Ni_{13}Zr$. Carbonyl group is altered in a more pronounced way with the elongation of 0.12 Å and 0.17 Å for the two catalysts, respectively.

Table 1. Unbinding energies of monohydrogenation products out of the complex with catalyst models Ni_{13} and $Ni_{13}Zr$ that were used to represent $NiTSNH_2$ and $NiZrTSNH_2$ catalysts, respectively.

Catalyst model	Product unbinding energy [kcal/mol]	
	CC-hydrogenation	CO-hydrogenation
Ni_{13}	45.2[a]	54.5[a]
$Ni_{13}Zr$	52.1	64.0

[a] Calculated with structures from Ref. 10

Addition of one H_2 molecule to the activated substrate yields two possible monohydrogenation products. Whereas for the Ni_{13} formation of both products is exothermic, zirconium doping makes hydrogenation of C=O bond mildly uphill in energy (ΔE = +0.3 kcal/mol). Formation of C=C hydrogenation product is in both cases exothermic (ΔE = -5.2 and -4.4 kcal/mol for Ni_{13} and $Ni_{13}Zr$, respectively). Energy spacing between the monohydrogenation products interacting with the catalyst models is about 4 kcal/mol for both catalysts studies and is smaller than energy spacing between isolated hydrogenation products (ca. 13 kcal/mol). Interestingly, unbinding energies of both possible products are very different for the two catalyst models (see Table 1). $Ni_{13}Zr$ interacts more strongly with the semihydrogeation products by about 7 – 10 kcal/mol so that it eases double hydrogenation.

Accepted Manuscript

This article is protected by copyright. All rights reserved.

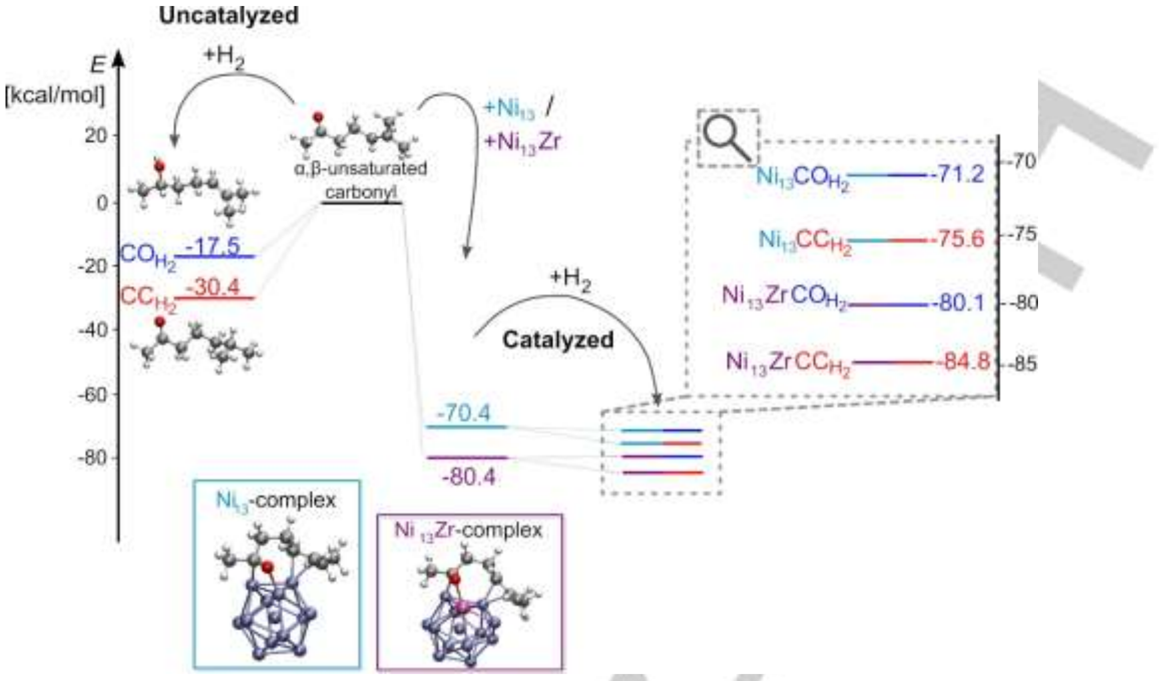

Figure 9. Relative energies (incl. zero-point energies) of reactants, intermediates and products of monohydrogenation reaction of the 6-methyl-5-hepten-2-one. Uncatalyzed reaction is shown for reference (left). In the presence of pure (represented with Ni_{13} structure) or Zr-doped ($Ni_{13}Zr$) the complex is formed that undergoes further hydrogenation reaction to form product bound to the catalyst molecule. Unbinding energies of the products are given in Table 1. Results for uncatalyzed and Ni13-catalyzed reaction were taken from Ref. 10.

Conclusions

Herein, we extended the on-the-fly protocol to Zr modification of parent Ni catalyst. The addition of zirconium led to a shift of the catalytic selectivity to the fully hydrogenated product also via the unsaturated alcohol reaction pathway, which is completely absent in the parent catalyst. The effect of Zr contrasts with what has been observed with Sn, in which we observed a clear switch in the thermodynamic order of the products. Comparison of XPS data for mono- and Zr-doped catalyst suggests that zirconium affects nickel electronic structure. According to theoretical calculations, the interaction model of the substrate with the catalyst species is similar for both undoped and doped catalysts, i.e. the interaction occurs via both C=O and C=C bonds. Additionally, Zr seems to gain a small positive charge while nickel decreases slightly its charge making it better Lewis acid centre than Ni and carbonyl oxygen prefer interaction with zirconium atom over nickel atom, resulting in a significant increase of the adsorption energy compared with the parent catalyst. It was also noted that the increase of the substrate flow rate increased the overall activity without affecting the process selectivity. This has been rationalized based on reversible surface poisoning by the substrate. On-the-fly modification coupled with spectroscopy and theoretical calculations is a powerful tool to evaluate and understand in real-time catalytic systems.

Experimental Section

Preparation of the catalysts

Synthesis of NiTSNH$_2$: Nickel catalyst (NiTSNH$_2$) was obtained at room temperature conditions, during one-pot, two-step synthesis. Firstly, Ni nanoparticles (Ni NPs) were collected by chemical reduction of Ni(II) acetylacetonate (0.001 mol) with $NaBH_4$ (molar ratio 1:2) in 65 ml of ethanol. To prevent agglomeration of Ni NPs, tenfold excess of trioctylophosphine oxide (TOPO) in relation to Ni was used. Synthesised NPs of Ni were subsequently immobilised on the commercial amino group terminated polymeric resin (TentaGel-S-NH$_2$, 5 g).

Synthesis of bimetallic Ni-Zr catalyst: Parent catalyst modification with zirconium was conducted in the H-Cube Pro™ continuous-flow system by surface organometallic modification chemistry (SOMC) methodology, similar as it was done for our previous work.[10] Briefly, 0.15 g of NiTSNH$_2$ was loaded in the stainless-steel cartridge (70 mm long, 4 mm i.d.) and pretreated for 1 h with 40 bar of hydrogen and ethanol flow. Subsequently, a solution of bis(cyclopentadienyl)dimethylzirconium(IV) ($ZrCp_2Me_2$) in ethanol ($3.17 \cdot 10^{-3}$ M) was flown through the cartridge at 100 °C under 40 bar of hydrogen with a flow rate of 0.5 ml/min for 10 min resulting in the preparation of NiZr$_{0.12}$TSNH$_2$. The obtained bimetallic catalyst was used in 6-methyl-5-hepten-2-one hydrogenation immediately after the preparation.

Accepted Manuscript

This article is protected by copyright. All rights reserved.

Catalysts characterisation

The metals concentration, both in monometallic and bimetallic catalyst was determined by atomic absorption spectrometry (AAS) after the dissolution of the metals in aqua regia.

Transmission electron microscopy (TEM) experiments were carried out on the electron microscope Titan G2 60 – 300 kV (FEI, Japan) equipped with EDAX EDS (energy-dispersive X-ray spectroscopy) detector. Microscopic studies of the catalysts were carried out at an accelerating voltage of the electron beam equal to 300 kV. The samples were prepared by their dispersing in pure alcohol using an ultrasonic cleaner and putting a drop of this suspension on carbon films on copper grids.

Powder X-ray diffraction (PXRD) measurements were performed employing Bragg-Brentano configuration. This type of arrangement was provided using PANalytical Empyrean diffraction platform, powered at 40 kV × 40 mA and equipped with a vertical goniometer, with theta-theta geometry using Ni filtered Cu Kα radiation. Data were collected in a range of $2\theta = 5 – 95°$, with a step size of 0.008° and counting time 60 s/step.

The chemical composition and chemical state of the catalyst samples were characterized by the X-ray photoelectron spectroscopy (XPS). XPS spectra were measured in a Microlab 350 spectrometer (Thermo Electron) using $Al_{K\alpha}$ ($h\upsilon = 1486.6$ eV, 300 W) as a source. Survey spectra and high-resolution spectra were recorded using 100 and 40 eV pass energy, respectively. A linear or Shirley background subtraction was made to obtain XPS signal intensity. The peaks were fitted using an asymmetric Gaussian/Lorentzian mixed function. Sample charging was corrected using C 1s *sp*^{3} signal (284.6 eV). The Ni and Zr signals were fitted using orbital doublet separations reported by NIST database.[22]

6-Methyl-5-hepten-2-one hydrogenation on the bimetallic catalyst

Catalytic hydrogenation on bimetallic catalyst was performed according to the same procedure as for NiTSNH$_2$[10] using ThalesNano H-Cube Pro™ continuous-flow micro-reactor. 6-methyl-5-hepten-2-one solution in ethanol ($5\cdot10^{-2}$ M) was flown through 0.15 g of a catalyst with a HPLC pump. The catalyst was placed in CatCart®70 cartridge. The hydrogen was generated *in situ* via water electrolysis. The catalytic reactions were conducted with over a wide range of temperatures (25 – 100 °C) and pressures (10 – 60 bar) but constant reactant flow rate (0.5 ml/min). Additionally, the flow rate influence on catalytic performance was analysed. Hence, two additional flow rates of reagents were tested: 0.3 and 1 ml/min. Substrate conversion and products formation were analysed by gas chromatography (GC), namely a Bruker 456 GC equipped with FID detector and non-polar BP-5 0.25 µm (5% phenyl, 95% dimethyl polysiloxane) column.

Quantum chemical calculations

Computational strategy was described in details in our previous study of nickel-tin catalyst.[10] Briefly, all computations were carried out within the density functional theory as implemented in ORCA 4.2.0 suite of programs.[23] We employed PBE gradient-corrected exchange-correlation functional[24] that was augmented with a posteriori dispersion correction of Grimme (D3).[25] Geometry optimizations and second derivative calculations used compact def2-SVP basis set, while triple-ζ def2-TZVP basis was chosen for single-point refinement.[26] All energy minima possess only positive normal modes. Final reported energies are thus PBE+D3/def2-TZVP and include zero-point energy correction. Global energy minimum geometry search of the $Ni_{13}Zr$ catalyst model was performed on the basis of Ni_{13} icosahedral minimum.[10] All multiplicities between 5 and 19 were considered. Cartesian coordinates of all relevant structures are provided in the Supplementary Information.

Acknowledgements

This work was partially supported by grant from the National Science Centre in Poland (OPUS 8, grant no. UMO-2014/15/B/ST5/02094) and the Polish Ministry of Science and Higher Education (IDEAS Plus II IdPII 2015000164). A.K. acknowledges support from the National Science Centre, Poland, grant number 2018/30/E/ST4/00004. Access to high performance computing resources was provided by the Interdisciplinary Centre for Mathematical and Computational Modelling in Warsaw, Poland, under grants no. G64-9 and GB77-11.

Conflicts of interest

There are no conflicts to declare.

Keywords: Chemoselective flow hydrogenation • 6-methyl-5-hepten-2-one • nano-Ni grafted on resin • on-the-fly catalyst modification • zirconium surface modification

[1] J. Yue, *Catal. Today*, **2018**, *308*, 3-19.
[2] I. Rossetti, *B. Catal. Today*, **2018**, *308*, 20-31.
[3] J. Sá, J. W. Medlin, *ChemCatChem*, **2019**, *11*, 3355-3365.
[4] K. Masuda, T. Ichitsuka, N. Koumura, K. Sato, S. Kobayashi, *Tetrahedron*, **2018**, *74*, 1705-1730.
[5] C. Paun, D. Giziński, M. Zienkiewicz-Machnik, D. Banaś, A. Kubala-Kukuś, J. Sá, *Catal. Commun.*, **2017**, *92*, 61-64.
[6] I. Goszwska, D. Giziński, M. Zienkiewicz-Machnik, D. Lisovytskiy, K. Nikiforov, J. Masternak, A. Śrębowata, J. Sá, *Catal. Commun.*, **2017**, *94*, 65-68.
[7] G. Vilé, N. Almora-Barrios, N. López, J. Pérez-Ramírez, *ACS Catal.*, **2015**, *5*, 3767-3778.
[8] D. Giziński, I. Goszewska, M. Zieliński, D. Lisovytskiy, K. Nikiforov, J. Masternak, M. Zienkiewicz-Machnik, A. Śrębowata, J. Sá, *Catal. Commun.*, **2017**, *98*, 17-21.
[9] D. Giziński, W. Błachucki, A. Śrębowata, M. Zienkiewicz-Machnik, I. Goszewska, K. Matus, D. Lisovytskiy, M. Pisarek, J. Szlachetko, J. Sá, *ChemCatChem*, **2018**, *10*, 3641-3646.
[10] M. Zienkiewicz-Machnik, I. Goszewska, A. Śrębowata, A. Kubas, D. Giziński, G. Słowik, K. Matus, D. Lisovytskiy, M. Pisarek, J. Sá, *Catal. Today*, **2018**, *308*, 38-44.
[11] J. P. Candy, B. Didillon, E. L. Smith, T. B. Shay, J. M. Basset, *J. Mol. Catal.*, **1994**, *86*, 179-204.
[12] L. Deghedi, J. M. Basset, J. P. Candy, J. A. Dalmon, A. C. Dubreuil, L. Fischer, *Chem. Engineer. Trans.*, **2009**, *17*, 31-36.
[13] S. V. Gribanova, Y. Y. Kharitonov, D. N. Dzhabarov, B. A. Rudenko, M. T. Yanotovskii, *Zh. Anal. Khim.*, **1990**, *45*, 1009-1016.
[14] D. McGinty, C. S. Letizia, A. M. Api, *Food Chem. Toxicol.*, **2010**, *48*, S82-S83.
[15] (a) S. O. Grim, L. J. Matienzo, W. E. Swartz Jr., *J. Am. Chem. Soc.*, **1972**, *94*, 51165117; (b) G. Ertl, R. Hierl, H. Knozinger, N. Thiele, H. P. Urbach, *Appl. Surf. Sci.*, **1980**, *5*, 49-64.

WILEY-VCH

Accepted Manuscript

This article is protected by copyright. All rights reserved.

[16] (a) K. S. Kim, N. Winograd, *Surf. Sci.*, **1974**, *43*, 625-643; (b) L. Salvati, L. E. Makovsky, J. M. Stencel, F. R. Brown, D. M. Hercules, *J. Phys. Chem.*, **1981**, *85*, 3700-3707; (c) K. Kishi, *J. Electron Spectrosc. Relat. Phenom.*, **1988**, *46*, 237-247.

[17] (a) B. P. Loechel, H. H. Strehblow, *J. Electrochem. Soc.*, **1984**, *131*, 713-723; (b) J. C. Klein, D. M. Hercules, *J. Catal.*, **1983**, *82*, 424-441.

[18] M. C. Biesinger, B. P. Payne, A. P. Grosvenor, L. W. M. Lau, A. R. Gerson, *Appl. Surf. Sci.*, **2011**, *257*, 2717-2730.

[19] X. Yu, F. Zhang, W. Chu, *RSC Adv.*, **2016**, *6*, 70537-70546.

[20] W. Song, P. Ma, J. Wang, W. Zhang, *Theor. Chem. Acc*., **2020**, *139*, 28.

[21] P.-O. Löwdin, *J Chem Phys*, **1950**, *18*, 365.

[22] https://srdata.nist.gov/xps/main_search_menu.aspx.

[23] F. Neese, *WIREs: Comp. Mol. Sci.*, **2017**, *8*, 1, e1327.

[24] J. P. Perdew, K. Burke, M. Ernzerhof, *Phys. Rev. Lett.*, **1996**, *77*, 3865-3868.

[25] S. Grimme, J. Antony, S. Ehrlich, H. Krieg, *J. Chem. Phys.*, **2010**, *132*, 154104.

[26] F. Weigend, R. Ahlrichs, *Phys. Chem. Chem. Phys.*, **2005**, *7*, 3297-3305.

WILEY-VCH

Accepted Manuscript

This article is protected by copyright. All rights reserved.

10.1002/cctc.202000235

Entry for the Table of Contents (Please choose one layout)

Layout 1:

FULL PAPER

On-the-fly protocol to optimize catalytic investigations by post-synthetic modification of nano-Ni catalyst morphology by introduction of zirconium is presented. The addition of small amounts of zirconium changes Ni ability to reduce C=C bond and significantly increases the concentration of other hydrogenation products, namely saturated and unsaturated alcohol.

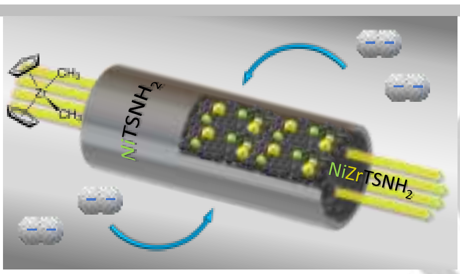

Małgorzata Zienkiewicz-Machnik, Ilona Goszewska, Damian Giziński, Anna Śrębowata, Katarzyna Kuzmowicz, Adam Kubas, Krzysztof Matus, Dmytro Lisovytskiy, Marcin Pisarek and Jacinto Sá**

Page No. – Page No.

Tuning nano-nickel catalyst hydrogenation aptitude by on-the-fly zirconium doping

WILEY-VCH

Accepted Manuscript

This article is protected by copyright. All rights reserved.